Magnetic correlations in the quasi-two-dimensional semiconducting ferromagnet $CrSiTe_3$

T. J. Williams,* A. A. Aczel, M. D. Lumsden, S. E. Nagler, and M. B. Stone
Quantum Condensed Matter Division, Neutron Sciences Directorate, Oak Ridge National Laboratory, Oak Ridge, Tennessee 37831, USA

J.-Q. Yan and D. Mandrus
Materials Science & Technology Division, Physical Sciences Directorate, Oak Ridge National Laboratory, Oak Ridge, Tennessee 37831, USA and Department of Materials Science & Engineering, University of Tennessee, Knoxville, Tennessee 37996, USA

(Received 27 March 2015; published 2 October 2015)

Intrinsic, two-dimensional ferromagnetic semiconductors are an important class of materials for overcoming the limitations of dilute magnetic semiconductors for spintronics applications. $CrSiTe_3$ is a particularly interesting member of this class, since it can likely be exfoliated down to single layers, where T_C is predicted to increase dramatically. Establishing the nature of the magnetism in the bulk is a necessary precursor to understanding the magnetic behavior in thin-film samples and the possible applications of this material. In this work, we use elastic and inelastic neutron scattering to measure the magnetic properties of single-crystalline $CrSiTe_3$. We find that there is a very small single ion anisotropy favoring magnetic ordering along the c axis and that the measured spin waves fit well to a model where the moments are only weakly coupled along that direction. Finally, we find that both static and dynamic correlations persist within the ab plane up to at least 300 K, strong evidence of this material's two-dimensional characteristics that are relevant for future studies on thin-film and monolayer samples.

DOI: 10.1103/PhysRevB.92.144404 PACS number(s): 75.30.Ds, 75.40.−s, 75.50.Pp, 85.75.−d

I. INTRODUCTION

The isolation of single layers of carbon atoms, in the form of graphene, resulted in the first physical realization of a true two-dimensional (2D) crystal leading to considerable study and revealing new physics [1]. The interest in graphene was not only fundamental, but also applied; potential device applications, such as spintronic devices, of such two-dimensional materials were recognized soon after the initial discovery [2]. Device applications of graphene are limited by its intrinsic properties, for instance, the lack of a band gap, and the search for 2D crystals soon extended to other materials. Spintronics requires semiconductors that possess ferromagnetic properties, particularly those that can be manipulated into one- or two-dimensional forms, so much work has focused on dilute magnetic semiconductors [3–6], which offer a large range of magnetic properties. These compounds have been the subject of much debate since their properties are highly dependent on epitaxial growth conditions, dopant distributions and even how the dopants are incorporated into the overall band structure [5]. In an effort to overcome these limitations, there has been an emergence of research into the much less common spintronic candidate: intrinsically ferromagnetic semiconductors [7,8]. The compound $CrSiTe_3$ belongs to this class, having an electronic band gap of 0.38 meV and a ferromagnetic transition at $T_C = 33$ K.

Much of the recent work on $CrSiTe_3$ has been in the form of theoretical calculations focused on the band structure and semiconducting properties, particularly calculations of the monolayer properties. Generalized gradient approximation (GGA) calculations on bulk $CrSiTe_3$ have calculated a bulk band gap of 0.6 meV, close to the experimental value, with the gap formed by the splitting of the Cr and Te levels [9]. These calculations correctly predict a ferromagnetic ground state that induces a slight spin polarization in the Si and Te atoms [9]. When the spins were assumed to be Ising-like and aligned along the c axis, local density approximation (LDA) calculations predicted a nearest-neighbor exchange $J = -0.58$ meV and transition temperature $T_C = 23$ K [10]. Experimentally, the structure has been determined in earlier work [11]. Hexagonal planes of Cr^{3+} ($S = 3/2$) atoms are stacked along the c axis, with each atom octahedrally coordinated by Te. The Te-Te bond lengths are ≈3.15 Å in the ab plane and ≈3.48 Å out of the plane, suggesting a very small octahedral distortion [11,12]. Previous neutron measurements also found a magnetic transition at 32.1 K corresponding to the Cr^{3+} moments ordering ferromagnetically along the c axis [13]. These measurements found a spin gap of nearly 6 meV, which was taken as evidence for Ising behavior. However, the inelastic measurements suffered from low statistics, which casts doubt on the accuracy of the determined magnetic dynamics. Additionally, they do not measure in multiple Brillouin Zones, making it possible that they have misidentified phonon modes as magnons. This offers an explanation as to why their measurements find three spin wave branches, a conclusion that is inconsistent with linear spin wave theory based on the known magnetic structure. Additionally, the claim that the spins are Ising-like cannot be conclusively derived from these measurements for the same reason. Other experimental work cited in that work does not contain evidence of Ising spins, since the cited magnetostriction measurements [14] are only dependent on the exchange anisotropy, while measurements of the single-ion anisotropy show it to be quite small [15,16]. Finally, the behavior of the magnetic correlations above T_C were only discussed qualitatively, leaving much room for a more accurate neutron scattering study to determine the magnetic correlations.

The resurgent interest in studying $CrSiTe_3$ has been driven by its applicability to spintronics. This has been prompted by

*williamstj@ornl.gov

the speculation that it may be possible to exfoliate the material down to single layers [8], which has been predicted to have the desirable effect of increasing the band gap to ≈0.59 eV [8] and the Curie temperature to ≈92 K [8,17]. These features have quickly created the need to understand the electronic and magnetic properties of $CrSiTe_3$.

II. EXPERIMENTAL DETAILS

$CrSiTe_3$ single crystals were grown using a self-flux technique, as previously reported [12]. $CrSiTe_3$ is rhombohedral, crystallizing in the space group R-3, which was confirmed with x-ray diffraction measurements on the samples used in this study. The crystal structure is shown in Fig. 1. Susceptibility measurements showed a ferromagnetic transition at $T_C = 33(1)$ K [12]. The large c/a ratio and the reasonably accessible magnetic transition make this a good candidate to study for its application as a two-dimensional spintronic material. In order to fully characterize the nature of the magnetic correlations, including their lower-dimensional properties, neutron scattering measurements were performed at the HB-3 and CG-4C (CTAX) triple axis spectrometers of the High-Flux Isotope Reactor, as well as the SEQUOIA time-of-flight spectrometer at the Spallation Neutron Source of the Oak Ridge National Laboratory.

Five single crystals of total mass 4.1 g and a mosaic of 2.25° were coaligned in the $[H\ 0\ L]$ scattering plane for use in the CTAX experiment. This array of single crystals was also used for the SEQUOIA experiment, while the largest single crystal (mass ≈1.2 g) was used for the HB-3 experiment, also aligned in the [H 0 L] scattering plane. The HB-3 measurements were performed in a closed-cycle refrigerator with a base temperature of 4.0 K using a fixed final energy of 14.7 meV. PG (002) monochromator and analyzer crystals were used with PG filters, and the collimation was 48'-40'-40'-120'. The SEQUOIA measurements were also performed in a closed-cycle refrigerator using fixed incident energies of 30 and 65 meV. The crystals were rotated in the [H 0 L] plane in 1° steps over an 83° range. The CTAX measurements were performed in a He-4 cryostat with a base temperature of 1.5 K using fixed final energies of 3 and 5 meV. This experiment used a PG002 monochromator, a Be filter and collimation settings of guide-open-80'-open.

III. ELASTIC NEUTRON SCATTERING

Figure 2(a) shows the temperature dependence of the (1 0 1) Bragg peak, which is both a nuclear and a magnetic peak, but the magnetic contribution is approximately ten times larger at 4 K. The red line is a fit to a critical exponent, which yields a transition temperature of 33.2(1) K and a critical exponent, $\beta = 0.151(12)$. This is close to the value expected for a two dimensional transition ($\beta_{2D,Ising} = 0.125$), and well below the values expected for a three dimensional transition ($\beta_{3D,Ising} = 0.326$ and $\beta_{3D,Heisenberg} = 0.367$). The low value of critical exponent is likely a consequence of strong two-dimensional correlations in this material. The long-range order below 33.2 K is, however, three-dimensional in nature, with the spins aligned ferromagnetically along the c-axis direction. This was confirmed by measuring 39 magnetic peaks in the $[H\ 0\ L]$ scattering plane, whose intensities below T_C were consistent with c-axis ordering. This is in agreement with previous work [13].

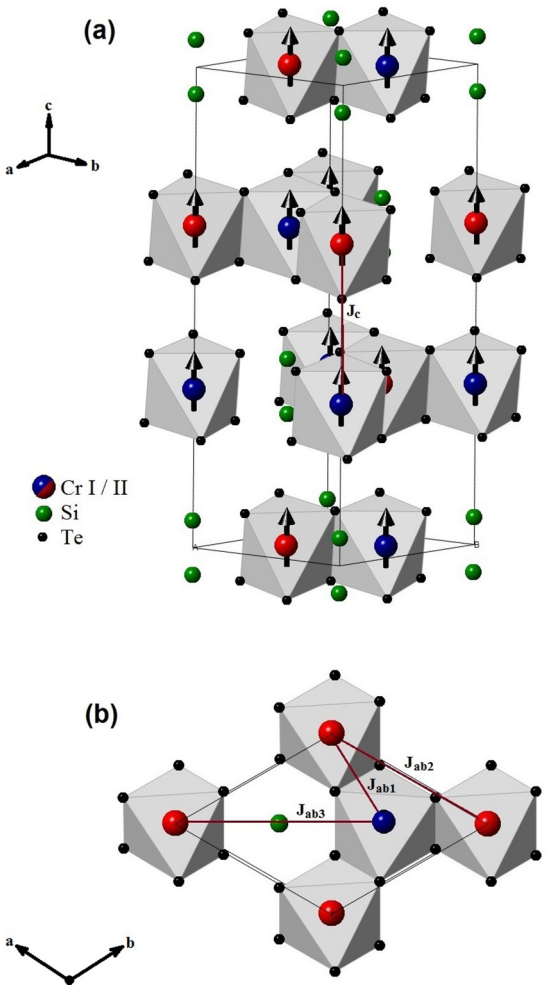

FIG. 1. (Color online) (a) The crystal structure of $CrSiTe_3$. The Cr^{3+} ions form hexagonal arrangements in the ab plane, which are then stacked along the c axis in an ABC-type stacking. This creates two magnetically inequivalent Cr sites, shown in red and blue. The Cr-I site (blue) has a Cr-II atom (red) above and a Si_2 pair (green) below, while it is reversed for the Cr-II site. Below $T_C = 33.2$ K, the Cr $S = 3/2$ spins align ferromagnetically along the c axis, due to a single-ion anisotropy, D_z. The nearest-neighbor exchanges out to 8 Å are shown in the figure, which includes three in-plane exchanges, J_{ab1}, J_{ab2}, and J_{ab3}, and one out-of-plane exchange J_c. (b) The structure of a single layer is shown, highlighting the different exchange interactions in this plane.

In addition to the magnetic diffraction peaks that emerge below T_C, diffuse scattering develops around the Bragg peaks, with an intensity that has a maximum at T_C, shown in the inset to Fig. 2(a). This diffuse scattering arises due to the in-plane correlations that are present, particularly above the ordering temperature. In order to study the magnetic correlations within the ab plane as a function of temperature, a series of two-axis measurements were performed on the HB-3 instrument. This was done by measuring along H about the wave vector (1 0 0.545), chosen such that the c axis was parallel to the

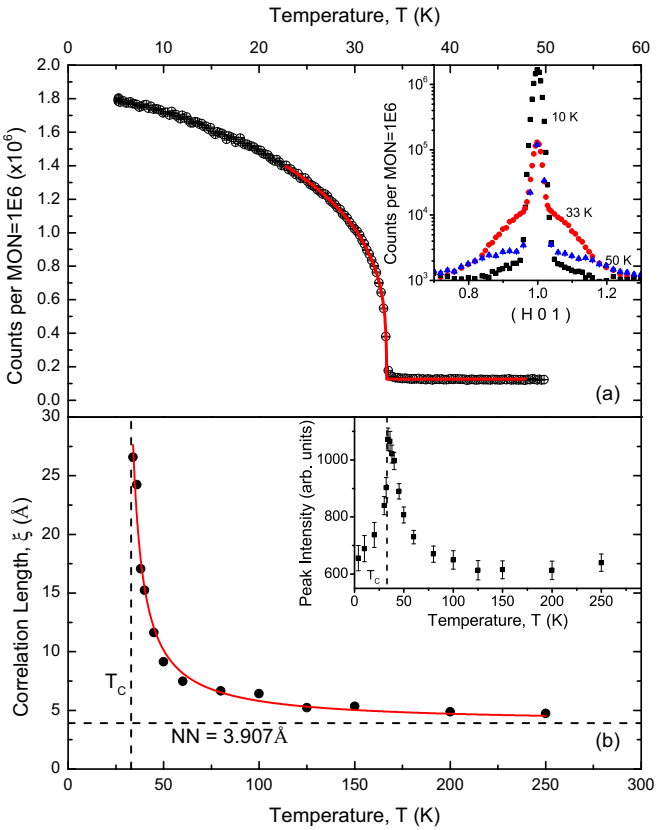

FIG. 2. (Color online) (a) The temperature dependence of the measured intensity at the (1 0 1) Bragg peak. This peak is both nuclear and magnetic, but the magnetic intensity is larger by approximately a factor of 10. A fit to this curve gives a transition temperature of $T_C = 33.2(1)$ K and a critical exponent $\beta = 0.151(12)$. (inset) Scans through the (1 0 1) Bragg peak along H at $T = 10$ (black squares), 33 (red circles), and 50 K (blue triangles), plotted on a logarithmic scale. This shows the sharp increase in the intensity at (1 0 1), corresponding to the 3D order, while the diffuse scattering, corresponding to the 2D correlations, is most intense at the transition. (b) The temperature dependence of the in-plane correlation length, determined from the two-axis scans described in the text. The line is a guide to the eye. We note that the in-plane correlation length is greater than the nearest-neighbor Cr-Cr distance at all temperatures measured, suggesting that the in-plane magnetic correlations are important well above the bulk ordering temperature.

final neutron wave vector, k_f [18,19]. The analyzer was then removed to integrate over various momentum transfers, but the $\hat{c} \parallel k_f$ orientation means that the component of the momentum transfer that varies with final energy is constrained to be along the L direction. This provides an accurate measure of the energy-integrated spin response for two-dimensional correlations within the ab plane.

The two-axis measurements are peaked at $H = 1$ for all temperatures measured and we find that the peak intensity is largest at T_C, which is shown in the inset to Fig. 2(b). The width of the peak can be used to calculate the in-plane correlation length, which is plotted in Fig. 2(b). As expected, the correlation length peaks at T_C, but decays as the temperature increases. This experiment did not have the required temperature stability or density of data points near T_C to perform an accurate measurement of the critical exponent, ν, or to observe the expected 2D to 3D crossover, which typically occurs within 0.01% to 0.1% of T_C [20]. However, we do observe that the correlation length remains larger than the nearest-neighbor distance at all temperatures measured, up to 250 K. This suggests that short-range correlations between the moments in the ab plane exist well above the ordering transition.

IV. SPIN WAVE MEASUREMENTS

Figures 3(a) and 3(c) show the spin wave dispersions measured on the SEQUOIA spectrometer, with an incident energy $E_i = 30$ meV. Panel (c) shows the dispersion along (0 0 L) with integration ranges of 0.4 reciprocal lattice units (r.l.u) along H and K. This shows that the dispersion is very weak along the c axis, and that the minimum in the spin wave dispersion is below 1 meV at the zone center, (0 0 −3). Since the dispersion along L is relatively weak, it was observed that varying the integration range along L had little effect on the plot of the spin wave spectrum. Therefore the spectrum shown in Fig. 3(a) was constructed by integrating over the full L range, $-12 \leqslant L \leqslant 12$, while using an integration range of 0.2 r.l.u. along K. This shows two spin wave bands, one peaking at ≈8 meV and the higher band peaking at ≈15 meV, which meet at the zone boundaries. The data along (H 0 0) using a smaller integration range for L showed identical dispersions, supporting the conclusion that the spin waves are close to two dimensional. The spin waves were modeled with a Hamiltonian given by

$$H = J_{ab1} \sum_i \vec{S}_i \cdot \vec{S}_{i+1} + J_{ab2} \sum_i \vec{S}_i \cdot \vec{S}_{i+2} + J_c \sum_i \vec{S}_i \cdot \vec{S}_{i+3} + J_{ab3} \sum_i \vec{S}_i \cdot \vec{S}_{i+4} - D_z \sum_i \left(\vec{S}_i^z\right)^2, \quad (1)$$

where the J's are exchange constants between neighboring spins $\vec{S}_i$ and D_z represents a single-ion anisotropy and the spins are assumed to be localized Cr^{3+}, $S = 3/2$ moments, as shown in Fig. 1. The very small value of the spin gap and the weak c-axis dispersion are both able to be accurately determined from the SEQUOIA data. The magnetic anisotropy necessitates a nonzero spin gap, but the SEQUOIA measurements have shown that it is less than 1 meV. This is consistent with magnetization data taken to characterize the sample, which observes very little magnetic hysteresis and a field of 1.5 T applied in the ab plane (the hard magnetization direction) is required to saturate the magnetic moment. Additionally, DFT calculations based on purely van der Waals interactions have found that there is an entropy difference of ≈20 μeV, favoring c-axis ordering, as compared to ordering within the ab plane [8,21]. This is very close to the value obtained for the single-ion anisotropy, as discussed below. The fits described below produce the simulations shown in Figs. 3(b) and 3(d). These show very good agreement with the experimental data, but we do observe a discrepancy at the nonzero integer values of H. At these points in the experimental data, we observe broadening of the optical mode and intensity shifts to the acoustic mode. These features are not seen in the simulation, though the origin of this difference is unclear.

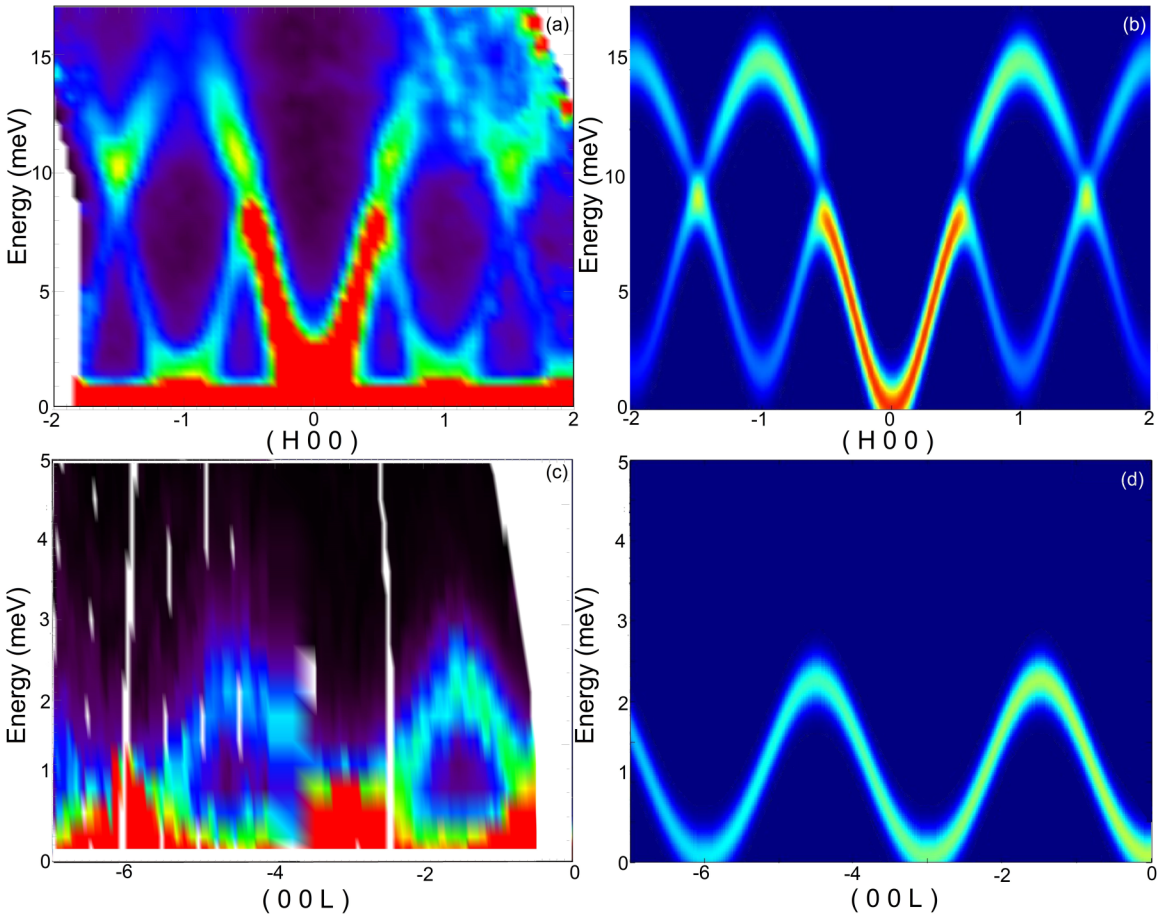

FIG. 3. (Color online) The panels on the left show the spin waves of $CrSiTe_3$ measured on the SEQUOIA spectrometer at $T = 10$ K, while the panels on the right show the calculated spin wave dispersions, along the (H 0 0) direction [(a) and (b)] and the (0 0 L) direction [(c) and (d)]. The calculated patterns use the model and exchange parameters described in the text, producing very good agreement with the experimental data.

In order to measure the magnitude of the spin gap and the dispersion out of the plane, measurements were performed on the cold neutron triple axis (CTAX) instrument at Oak Ridge National Laboratory. The energy resolution of a constant-Q scan was insufficient to separate the gapped mode from the elastic scattering. To extract the spin gap value, a series of constant-E scans was performed, shown in Fig. 4(a). These scans focus on the region near the zone center (0 0 3), where a spin gap is expected in the spectrum. By assuming that the energy of the spin waves, $E \propto |q|^2$ in the long-wavelength limit, we can extract an approximate measure of the gap, despite it being within the resolution of the

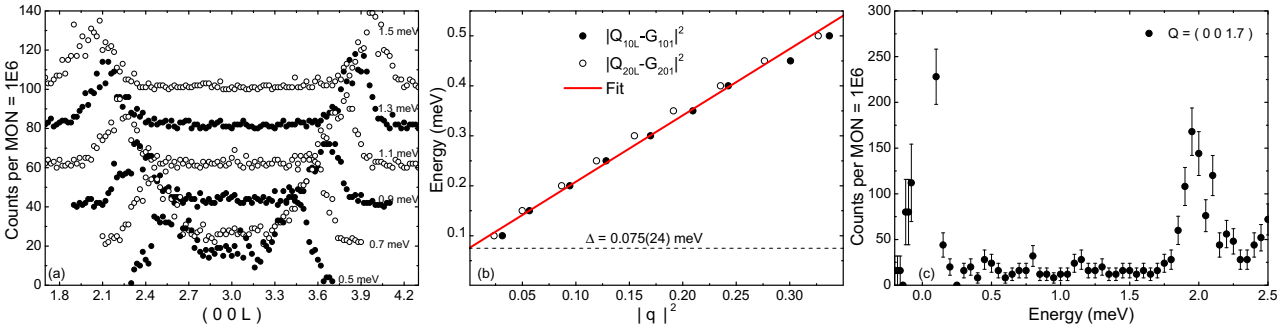

FIG. 4. (Color online) (a) The constant-E scans measured on the Cold Triple-Axis (CTAX) Spectrometer at 1.5 K along (0 0 L), which are offset along the y axis for clarity. These scans focus on the region near the zone center (0 0 3), where a spin gap is expected in the spectrum. By assuming that the energy of the spin waves, $E \propto |q|^2$ in the long-wavelength limit, we can extract an approximate measure of the gap, despite it being within the resolution of the instrument. (b) The q dependence of the spin waves near the zone center is plotted, showing q^2 dependence. A fit to these values gives a value for the gap $\Delta = 0.075(24)$ meV. (c) A constant-$\vec{Q}$ measurement at $\vec{Q} = (1.700)$ near the zone boundary, (0 0 1.5), allows for a determination of the value of the out-of-plane coupling, $J_c = -0.730(96)$ meV.

TABLE I. The exchange constants obtained from fitting the inelastic measurements using Eq. (1). To properly describe the spin waves, it was necessary to use couplings up to 8 Å, which requires three in-plane interactions and one out-of-plane. Consistent with the quasi-2D nature of the material, the value of J_c gives a very small dispersion along the c axis and, as expected from the very small octahedral distortion, the value of the single-ion anisotropy D_z is very close to zero.

Exchange	Description	Distance	Value (meV)
J_{ab1}	first NN in-plane	3.907 Å	− 1.27(23)
J_{ab2}	second NN in-plane	6.768 Å	− 0.10(50)
J_{ab3}	third NN in-plane	7.814 Å	− 0.285(73)
J_c	first NN out-of-plane	6.852 Å	− 0.730(96)
D_z	Single ion anisotropy		0.0252(80)

instrument. The data were fit in multiple zones, as shown in Fig 4(b), showing q^2 dependence. This gave a value of the spin gap, $\Delta = 0.075(24)$ meV, allowing a measurement of the single-ion anisotropy, $D_z = \Delta/2S = 0.0252(80)$ meV. The single-ion anisotropy arises from the small c-axis distortion in the Te octahedra surrounding the Cr^{3+} ions. This nearly perfect octahedral environment makes spin-orbit effects very weak and the Cr-Cr bond is a point of local centrosymmetry, ruling out Dyaloshinskii-Moriya interactions as an origin for the energy gap. This small gap is consistent with theoretical predictions that the energy difference between c-axis and ab-plane ordering is less than 0.1 meV. Constant-$\vec{Q}$ measurements near the zone boundary, (0 0 1.5), shown in Fig. 4(c), allow us to determine the value of the out-of-plane coupling, J_c, since the energy of the lower spin wave branch along L depends only on D_z and J_c. Using the value of D_z determined above, we obtain $J_c = -0.730(96)$ meV.

These values were then fixed for the purposes of fitting the SEQUOIA data to obtain the in-plane exchange constants. The fitting was performed using the fitting routines built into the HORACE software package [22], which used the dispersions calculated by SPINW [23] as its model, comparing the intensities of the data and calculation over the entire range in the $\vec{Q}$-E slice. This allowed the in-plane exchange constants to be fit simultaneously, utilizing the two-dimensional data set shown in Fig. 3(a). The values of these three exchange constants obtained from fitting the data shown in Fig. 3(a) to Eq. (1), as well as those determined from the CTAX measurements, are given in Table I.

As expected for a quasi-two-dimensional system, the nearest-neighbor in-plane coupling, J_{ab1}, is the dominant interaction and is ferromagnetic, as are the other in-plane exchange constants. While J_{ab1} is only slightly larger than J_c, there are three nearest neighbors in the ab plane compared to only one along the c axis. This makes the in-plane exchange more than five times larger than the out-of-plane coupling. The ferromagnetic origin of the in-plane terms is likely due to superexchange mediated by the Te ions, shown in Fig. 1(b). The Cr^{3+} ion direct exchange is antiferromagnetic, though the large nearest-neighbor Cr-Cr distance of 3.987 Å should make this a weak effect [24,25]. Finally, the Cr octahedra are edge-sharing and the Cr-Te-Cr angle is 88.8°, very close to perfectly orthogonal. This arrangement of the ions would suggest that superexchange of the type described by the Goodenough-Kanamori rules [26–28] would be ferromagnetic, consistent with the observations of ferromagnetism in other layered Cr^{3+} compounds with similar superexchange pathways [25]. First-principles DFT calculations on monolayer $CrSiTe_3$ suggest that the second and third nearest-neighbor in-plane interactions are Cr-Te-Te-Cr double-superexchange interactions [17], leading to the small values we observe for J_{ab2} and J_{ab3}. Furthermore, the observation that $|J_{ab2}| < |J_{ab3}|$ was also predicted by the DFT calculations. There are two double-superexchange pathways that contribute to J_{ab2}, one of which is ferromagnetic and the other antiferromagnetic, making it a very weak exchange [17].

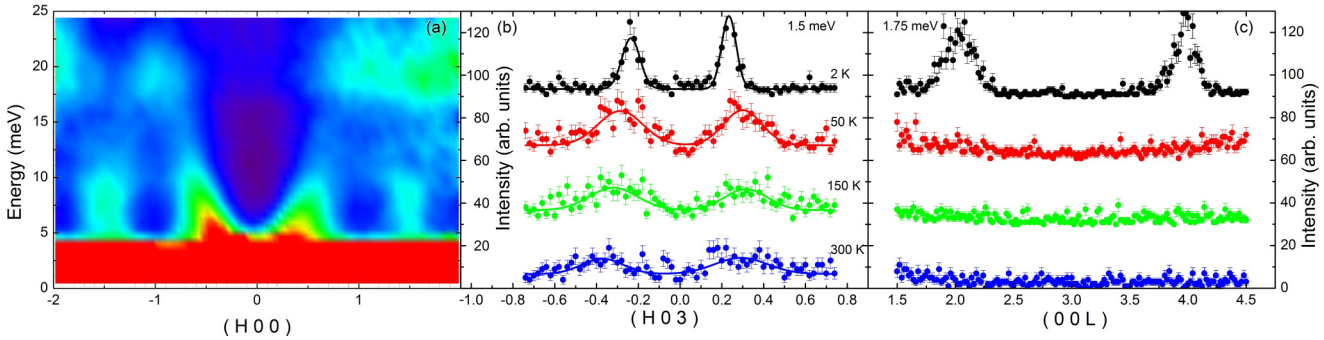

FIG. 5. (Color online) The temperature dependence of spin dynamics. (a) The inelastic neutron spectrum measured at $T = 40$ K on the SEQUOIA spectrometer. We see that broadened spin wave features remain, even above the transition, while there are no such excitations along the L direction. This is a clear signature of the two-dimensionality of this material. The feature at 20 meV is extrinsic to the sample, verified by performing an empty can measurement. (b) The in-plane spin dynamics along (H 0 3) at various temperatures, measured on CTAX and offset for clarity. Sharp spin waves are observed below the transition, but dynamic correlations exist at all temperatures measured. The high-temperature features are reminiscent of the spin waves seen below T_C, but significantly broadened. The lines are guides to the eye. (c) In contrast, there are no dynamic correlations along the L direction above T_C (also shown offset for clarity). This suggests that three-dimensional correlations only exist below the Curie temperature, while the in-plane dynamic correlations persist up to at least 300 K.

The neutron scattering measurements are also consistent with the theoretical predictions of an enhanced transition temperature in $CrGeTe_3$ and $CrSnTe_3$, as well as monolayer $CrSiTe_3$ [8,17,21]. Despite the spins being only weakly Ising-like, the easy-axis spin anisotropy created by the imperfect Te octahedra still allows for ordering in two-dimensions, such as when the materials are reduced to monolayers. The loss of the out-of plane coupling is compensated by an increased in-plane ferromagnetic exchange, as predicted by several theoretical studies that compare bulk $CrSiTe_3$ to its monolayer version and the chemically substituted $CrGeTe_3$ and $CrSnTe_3$ [8,17,21]. The increased ferromagnetic exchange within the *ab*-plane arises due to the increase of the nearest-neighbor Cr-Cr distance in all of these cases. This serves to reduce the Cr-Cr direct exchange, which is antiferromagnetic, while pushing the Cr-Te-Cr bond angle closer to 90°. This increases the effect of the ferromagnetic superexchange, resulting in the increased values of T_C [25].

Inelastic neutron scattering measurements performed above the ferromagnetic transition are shown in Fig. 5. Measurements at 40 K along the (H 0 0) direction are presented in Fig. 5(a). These data indicate that the spin waves are still present within the planes, but have been significantly broadened. The minima in the spin waves seen at (1 0 0) and (2 0 0) in Fig. 3(a) have disappeared, as they arose from the weak dispersion along the L direction. This indicates that there is no dispersion along L above T_C, and these broadened spin waves are only present within the *ab* planes at these temperatures. To track the temperature evolution of the spin waves, constant-E measurements were performed along (H 0 0) at $E = 1.75$ meV and (0 0 L) at $E = 1.5$ meV as a function of temperature. These are shown in Figs. 5(b) and 5(c), respectively. We see that the spin waves along L disappear abruptly above T_C, but that the broadened spin waves exist at the same $\vec{Q}$ along (H 0 0) well above the ordering transition, up to at least 300 K.

V. CONCLUSIONS

We have measured $CrSiTe_3$ using elastic and inelastic neutron scattering. These measurements observe bulk ferromagnetism below $T_C = 33.2(1)$ K and the critical exponent of the neutron scattering intensity was found to be $\beta = 0.151(2)$, close to the value expected for a two-dimensional system. The magnetic Bragg peaks also exhibited a diffuse component, the intensity of which peaks at T_C, indicating two-dimensional ferromagnetic correlations are present in the *ab* plane above the ferromagnetic transition. To characterize these correlations, two-axis measurements were performed, which provided an effective quantitative measure of the in-plane correlation length. As expected, the correlation length diverged at T_C but was still larger than the nearest-neighbor Cr-Cr distance at all temperatures measured, up to 250 K. These measurements suggest that while $CrSiTe_3$ only orders in three dimensions below 33 K, there are strong two-dimensional static correlations that persist up to at least room temperature.

In contrast to the previous assumption of Ising spins, the spin wave measurements suggest that the spins are very Heisenberg-like, with a very small spin gap of 0.075(24) meV due to a small single-ion anisotropy. X-ray diffraction measurements [12] and DFT calculations [21] find evidence of van der Waals interactions creating a very small octahedral distortion along the c axis, creating the anisotropy. We find that the dominant interaction, $J_{ab1} = -1.27(23)$ meV, is likely due to the superexchange mediated by the Te ions. The second and third nearest-neighbor in-plane interactions are much weaker, likely a result of double-superexchange interactions.

Above T_C, no spin waves are present along the L direction, but they persist in a broadened form along the H direction. Measurements at 40 K along (H 0 0) showed broadened spin waves consistent with dynamics confined to the *ab* planes, a clear indication of two-dimensional behavior, while temperature-dependent measurements show an inelastic signal that is visible up to 300 K. The latter finding suggests that there are dynamic in-plane correlations that persist up to at least room temperature as well. Considering these results in conjunction with the neutron diffraction measurements, we find that both static and dynamic in-plane magnetic correlations exist up to at least 300 K, ten times T_C. This illustrates the importance of two-dimensional correlations in these materials and may suggest that similar physics is relevant in the isostructural compounds $CrGeTe_3$ and $CrSnTe_3$, as well as for monolayer $CrSiTe_3$, where it has been predicted that increased separation or complete decoupling of the hexagonal Cr layers puts an increased emphasis on the two-dimensional correlations. Taken together with the dramatic increase in the magnetic transition temperature driven by a separation of the intralayer Cr atoms in these materials, this suggests that spintronic devices [2] that make use of these semiconductors on a substrate that enhances the magnetic character through strain or other effects may be capable of supporting intrinsic ferromagnetism at temperatures approaching, or even surpassing, room temperature.

ACKNOWLEDGMENTS

We acknowledge instrument support from S. Chi, T. Hong, and J. Niedziela. This research at ORNL's High Flux Isotope Reactor and Spallation Neutron Source was sponsored by the Scientific User Facilities Division, Office of Basic Energy Sciences, US Department of Energy. T.J.W. acknowledges support from the Wigner Fellowship program at Oak Ridge National Laboratory. D.G.M and J.-Q.Y. acknowledge support from NSF DMR 1410428. This manuscript has been authored by UT-Battelle, LLC under Contract No. DE-AC05-00OR22725 with the U.S. Department of Energy. The United States Government retains and the publisher, by accepting the article for publication, acknowledges that the United States Government retains a nonexclusive, paid-up, irrevocable, world-wide license to publish or reproduce the published form of this manuscript, or allow others to do so, for United States Government purposes. The Department of Energy will provide public access to these results of federally sponsored research in accordance with the DOE Public Access Plan (http://energy.gov/downloads/doe-public-access-plan).

[1] A. K. Geim and K. S. Novoselov, Nature (London) **6**, 183 (2007).
[2] W. Han, R. K. Kawakami, M. Gmitra, and J. Fabian, Nat. Nanotechnol. **9**, 794 (2014).
[3] I. Zutic, J. Fabian, and S. Das Sarma, Rev. Mod. Phys. **76**, 323 (2004).
[4] A. H. MacDonald, P. Schiffer, and N. Samarth, Nat. Mater. **4**, 195 (2005).
[5] T. Dietl, Nat. Mater. **9**, 965 (2010).
[6] Z. Deng, C. Q. Jin, Q. Q. Liu, X. C. Wang, J. L. Zhu, S. M. Feng, L. C. Chen, R. C. Yu, C. Arguello, T. Goko, F. Ning, J. Zhang, Y. Wang, A. A. Aczel, T. Munsie, T. J. Williams, G. M. Luke, T. Kakeshita, S. Uchida, W. Higemoto, T. U. Ito, B. Gu, S. Maekawa, G. D. Morris, and Y. J. Uemura, Nat. Commun. **2**, 422 (2011).
[7] N. S. Rogado, J. Li, A. W. Sleight, and M. A. Subramanian, Adv. Mater. **17**, 2225 (2005).
[8] X. Li and J. Yang, J. Mater. Chem. C **2**, 7071 (2014).
[9] S. Lebègue, T. Björkman, M. Klintenberg, R. M. Nieminen, and O. Eriksson, Phys. Rev. X **3**, 031002 (2013).
[10] B. Siberchot, S. Jobic, V. Carteaux, P. Gressier, and G. Ouvrard, J. Phys. Chem. **1996**, 5863 (1996).
[11] G. Ouvrard, E. Sandre, and R. Brec, J. Solid State Chem. **73**, 27 (1988).
[12] L. Casto, A. J. Clune, M. O. Yokosuk, J. L. Musfeldt, T. J. Williams, H. L. Zhuang, M. W. Lin, K. Xiao, R. G. Hennig, B. C. Sales, J.-Q. Yan, and D. Mandrus, APL Mat. **3**, 041515 (2015).
[13] V. Carteaux, F. Moussa, and M. Spiesser, Europhys. Lett. **29**, 251 (1995).
[14] A. Herpin, *Théorie du Magnetisme* (INSTN-PUF, Paris, 1968), pp. 158, 356.
[15] A. Abragam and B. Bleaney, *Electron Paramagnetic Resonance of Transition Ions* (Caredon Press, Oxford University Press, Oxford, 1969).
[16] L. J. de Jongh, *Magnetic Properties of Layered Transition. Metal Compounds* (Kluwer, Dordrecht, 1990), p. 230.
[17] N. Sivadas, M. W. Daniels, R. H. Swendsen, S. Okamoto, and D. Xiao, Phys. Rev. B **91**, 235425 (2015).
[18] R. J. Birgeneau, H. J. Guggenheim, and G. Shirane, Phys. Rev. B **1**, 2211 (1970).
[19] J. Als-Nielsen, R. J. Birgeneau, H. J. Guggenheim, and G. Shirane, Phys. Rev. B **12**, 4963 (1975).
[20] A. Taroni, S. T. Bramwell, and P. C. W. Holdsworth, J. Phys.: Condens. Matter **20**, 275233 (2008).
[21] H. L. Zhuang, Y. Xie, P. R. C. Kent, and P. Ganesh, Phys. Rev. B **92**, 035407 (2015).
[22] T. G. Perring *et al.*, HORACE: Software for Visualising and Manipulating S(Q, w) Measured in all Four Dimensions, http://horace.isis.rl.ac.uk. Accessed 18 March 2015.
[23] S. Toth and B. Lake, arXiv:1402.6069.
[24] P. Colombet and M. Danot, Solid State Commun. **45**, 311 (1983).
[25] K. Motida and S. Miyahara, J. Phys. Soc. Jpn. **28**, 1188 (1970).
[26] J. B. Goodenough, Phys. Rev. **100**, 564 (1955).
[27] J. B. Goodenough, J. Phys. Chem. Solids **6**, 287 (1958).
[28] J. Kanamori, J. Phys. Chem. Solids **10**, 87 (1958).